Article

Stability Computations for Isomers of La@C$_n$ (n = 72, 74, 76)

Zdeněk Slanina [1,*], **Filip Uhlík** [2], **Shyi-Long Lee** [3], **Ludwik Adamowicz** [4], **Takeshi Akasaka** [1] and **Shigeru Nagase** [5]

[1] Life Science Center of Tsukuba Advanced Research Alliance, University of Tsukuba, 1-1-1 Tennodai, Tsukuba, Ibaraki 305-8577, Japan; E-Mail: akasaka@tara.tsukuba.ac.jp

[2] Department of Physical and Macromolecular Chemistry, Charles University in Prague, Faculty of Science, Albertov 6, 128 43 Praha 2, Czech Republic; E-Mail: filip.uhlik@natur.cuni.cz

[3] Department of Chemistry and Biochemistry, National Chung-Cheng University, Chia-Yi 62117, Taiwan; E-Mail: chesll@ccu.edu.tw

[4] Department of Chemistry, University of Arizona, Tucson, AZ 85721-0041, USA; E-Mail: ludwik@email.arizona.edu

[5] Fukui Institute for Fundamental Chemistry, Kyoto University, Nishihiraki-cho 34-4, Kyoto 606-8103, Japan; E-Mail: nagase@ims.ac.jp

* Author to whom correspondence should be addressed; E-Mail: zdenek@ims.ac.jp; Tel.: +81-564-53-3258-3922; Fax: +81-564-53-3258-3925.

Abstract: Density-functional theory calculations are presented for low-energy La@C$_{72}$, La@C$_{74}$ and La@C$_{76}$ isomers with IPR (isolated pentagon rule) and non-IPR cages. The relative isomeric production yields at high temperatures are evaluated using the calculated terms, and the relationships to observations are discussed.

Keywords: metallofullerenes; DFT computations; isomeric stabilities; Gibbs-energy evaluations; IPR and non-IPR fullerene cages

1. Introduction

There are only two species [1,2] among C$_{60}$–C$_{96}$ empty fullerenes that are not yet isolated—C$_{72}$ and C$_{74}$. However, their metallofullerenes are well known—for example Ca@C$_{72}$ [3], La@C$_{72}$ [4], Ca@C$_{74}$ [5], Sm@C$_{74}$ [6], Sr@C$_{74}$ [7], Ba@C$_{74}$ [8], La@C$_{74}$ [9,10], Eu@C$_{74}$ [11], Yb@C$_{74}$ [12],

$Sc_2@C_{74}$ [13] or $Er_3@C_{74}$ [14]. Among them, $La@C_{72}$ and $La@C_{74}$ have a special position as their X-ray crystallographic analysis is available [4,10], though for solvent-related derivatives, namely $La@C_{72}$-$C_6H_3Cl_2$ with a non-IPR (IPR: isolated pentagon rule [15]) carbon cage and $La@C_{74}$-$C_6H_3Cl_2$ (IPR cage). Finally, while $La@C_{76}$ has also been observed [16,17], its cage structure is not yet known.

The metallofullerenes based on the C_n (n = 72, 74, 76) cages have also been computed [18–26]. The first relative isomeric stabilities were evaluated [21,22] for $Ca@C_{72}$ and $Ca@C_{74}$ and it was shown that the non-IPR encapsulations are significant only in $Ca@C_{72}$. The present paper deals with such calculations for $La@C_{72}$, $La@C_{74}$ and $La@C_{76}$, consistently using the Gibbs energies as required by high temperatures [27–30].

2. Calculations

There is [17] just one IPR isomer for C_{72} (D_{6d}) and C_{74} (D_{3h}) while there are two IPR isomers for C_{76} (D_2 and T_d symmetry). In addition, a few relevant (most populated) non-IPR cages are considered here (the cages are labeled by some conventional code numbers or by symmetry groups).

The geometry optimizations were carried out using density functional theory (DFT), namely employing Becke's three parameter functional [31] with the non-local Lee–Yang–Parr correlation functional [32] (B3LYP, as we deal with open-shell systems—the unrestricted B3LYP, or UB3LYP, treatment is applied) in the combined basis set of the 3–21G basis for C atoms and a dz basis set for La suggested by Hay and Wadt [33] with the effective core potential (denoted here by 3–21G∼dz). The B3LYP/3–21G∼dz geometry optimizations were carried out with the analytically constructed energy gradient as implemented in the Gaussian 03 program package [34].

In the optimized B3LYP/3–21G∼dz geometries, the harmonic vibrational analysis was carried out with the analytical force-constant matrix. In the same B3LYP/3–21G∼dz optimized geometries, higher-level single-point energy calculations were also performed, using the standard 6–31G* basis set for C atoms, *i.e.*, the B3LYP/6–31G*∼dz level. Moreover, the SDD (Stuttgart/Dresden) basis set [35] was also employed (with the SDD effective core potential for La) for comparison. The Gibbs energies were evaluated using the rotational-vibrational partition functions constructed [36] from the calculated structural and vibrational data using the rigid rotator and harmonic oscillator (RRHO) approximation. Although the temperature region where fullerene or metallofullerene electric-arc synthesis takes place is not yet known, the new observations [37] supply some arguments to expect it to be around or above $1500\,K$. Thus, the computed results discussed here are also focused on the temperature region.

Relative concentrations (mole fractions) x_i of m isomers can be evaluated [36] through their partition functions q_i and the enthalpies at the absolute zero temperature or ground-state energies $\Delta H_{0,i}^o$ (*i.e.*, the relative potential energies corrected for the vibrational zero-point energies) by a compact formula:

$$x_i = \frac{q_i \exp[-\Delta H_{0,i}^o/(RT)]}{\sum_{j=1}^m q_j \exp[-\Delta H_{0,j}^o/(RT)]} \tag{1}$$

where R is the gas constant and T is the absolute temperature. Equation (1) is an exact formula that can be directly derived [36] from the standard Gibbs energies of the isomers, supposing the conditions of the inter-isomeric thermodynamic equilibrium. The electronic partition functions for Equation (1) were constructed by direct summation of the TD B3LYP/3-21G∼dz electronic excitation energies.

However, the isomeric populations are not very sensitive to the electronic contributions, and therefore the vibrational-rotational partition functions for the electronic excited states are taken as equal to those of the ground state. The chirality contribution was included accordingly [38].

Let us note that in addition to the conventional RRHO treatment in Equation (1), a further modified approach for the description of the encapsulate motions can be considered [39], following the findings [40] that the encapsulated atoms can exercise large amplitude motions, especially so at elevated temperatures (unless the motions are restricted by cage derivatizations [41]). One can expect that if the encapsulate is relatively free, then at sufficiently high temperatures its behavior in different cages will bring about the same contribution to the partition functions. However, such uniform contributions would then cancel out in Equation (1). This simplification is called [39] the free, fluctuating, or floating encapsulate model (FEM) and requires two steps. In addition to the removal of the three lowest vibrational frequencies (belonging to the metal motions in the cage), the symmetries of the cages should be treated as the highest (topologically) possible, which reflects the averaging effects of the large amplitude motions. For example, for the C_{74} IPR isomer species, the D_{3h} symmetry is employed within the FEM scheme, although its statical symmetry (*i.e.*, after the geometry optimization) is just C_{2v}. Generally, the FEM treatment gives a better agreement [42] with the available observed data than the RRHO approach.

3. Results and Discussion

Table 1 presents the separation energetics for the three La@C_{72} isomers (Figure 1). As the sole IPR species is considerably higher in energy, it is not significantly populated even at very high temperatures (Figure 2). Although the potential energy difference is very small between the C_{2v} and C_2 non-IPR isomers, the C_2-cage-based La@C_{72} structure is always more populated and the C_2 cage is indeed present in the observation [4] (as the only isomer isolated). The effects of the cage derivatizations during chromatographic separation should however also be evaluated as a final step in theory-experiment comparisons. The relative-stability picture is basically the same from the FEM and RRHO treatments as the two decisive non-IPR species do have the same symmetry number in both approaches. The IPR-cage-based La@C_{72} is somewhat more populated in the RRHO approximation owing to symmetry number reduction, but still remains as a very minor isomer.

Table 1. La@C_{72} relative potential energies $\Delta E_{pot,rel}$ computed [a] in the B3LYP/3–21G$\sim$dz optimized geometries.

Species [b]	$\Delta E_{pot,rel}$	(kcal/mol)
	B3LYP/3–21G$\sim$dz	B3LYP/6–31G$^*\sim$dz
IPR	36.80	37.40
C_{2v}	4.40	0.26
C_2	0	0

[a] See the text for the abbreviations; [b] See Figure 1.

Figure 1. B3LYP/3–21G∼dz optimized structures of the three studied La@C$_{72}$ isomers.

D_{6d} IPR $\qquad\qquad$ C_{2v} $\qquad\qquad$ C_2
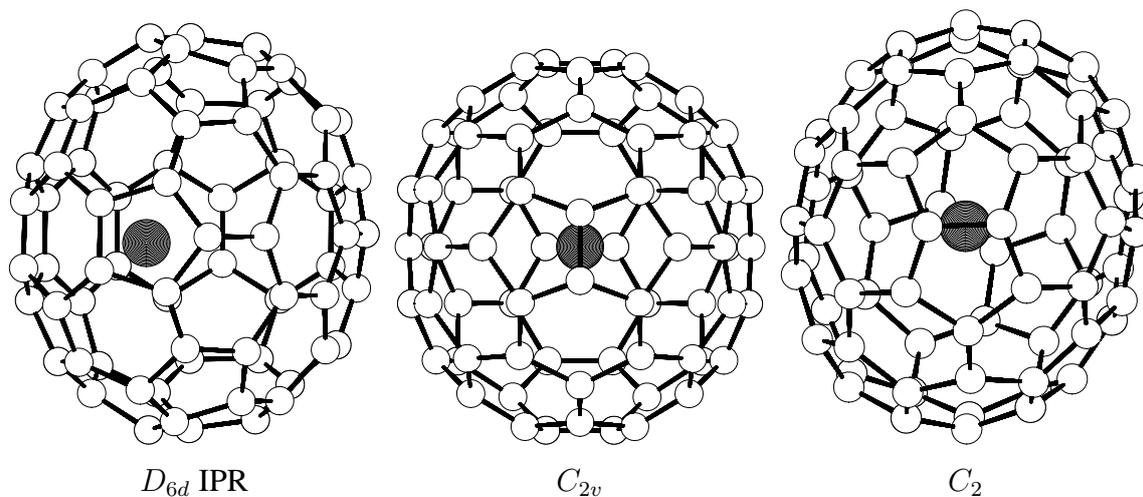
Figure 2. Relative concentrations of the La@C$_{72}$ isomers computed with the B3LYP/6–31G*∼dz energetics, B3LYP/3–21G∼dz entropy, and FEM treatment.
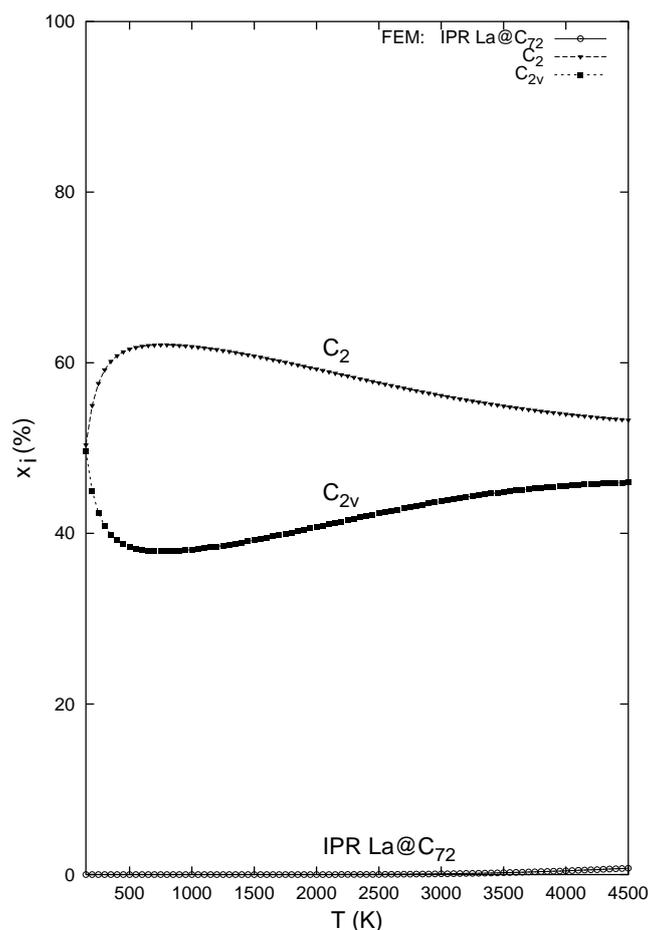
The role of the sole IPR cage is however quite different in the La@C$_{74}$ isomeric system. The La@C$_{74}$ isomer with the IPR cage (Figure 3) is the lowest in energy [25] and the non-IPR species are located rather high. Temperature developments of the relative concentrations of the three La@C$_{74}$ isomers in the RRHO and FEM treatments are presented in Figure 4—it is a system where the populations from

the two approaches are considerably different. In the temperature region around $1500\,\text{K}$, the D_{3h} species is clearly prevailing while two non-IPR cage related isomers 103 and 4 represent just a few percent of the equilibrium isomeric mixture. The pronounced difference between the RRHO and FEM treatments is substantially related to the considerable change in the symmetry number of the IPR-cage-based endohedral (from 2 in the rigid RRHO to 6 in the flexible FEM approach). Still, both evaluations are in agreement with the observation [10] in which just one La@C_{74} species was isolated and evidenced by X-ray analysis to contain the IPR carbon cage. According to the calculations, the La endohedrals with non-IPR C_{74} cages could possibly be isolated only with a considerable separation effort (though the derivatization effects by solvent are yet to be evaluated).

Figure 3. B3LYP/3-21G∼dz optimized structure of the observed La@C_{74} IPR-based isomer.

D_{3h} IPR
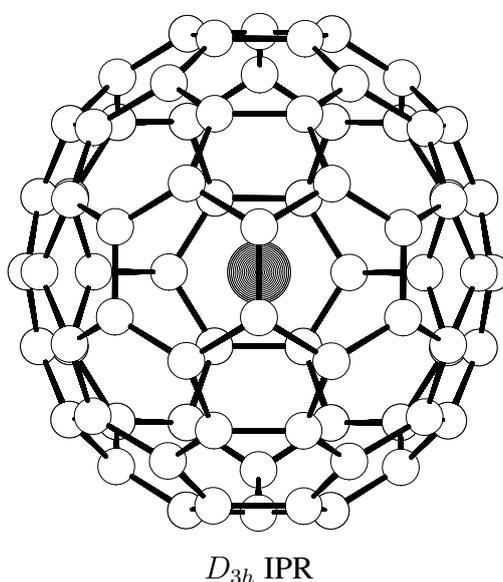
The sensitivity to the symmetry representation is even larger in the La@C_{76} isomeric set (Figure 5)—owing to the effective T_d symmetry of the lowest energy species (Table 2) in the FEM approach. Interestingly enough, La encapsulation into the other IPR cage (D_2) produces an endohedral higher by some $20\,\text{kcal/mol}$ so that it cannot compete with structure 6244 and a few other non-IPR La@C_{76} isomers (Table 2). Figure 6 demonstrates that while the T_d-IPR-based endohedral is the major isomer in the relevant temperature region, there should be a significant minor isomer, namely derived from the 6244 cage, and possibly even a second minor species related to the 6247 non-IPR cage. However, this computational prediction remains to be checked by observations. Thus, in the studied triad of isomeric systems, La@C_{76} comes rather in the middle, between La@C_{72} as non-IPR controlled and La@C_{74} just the opposite.

Figure 4. Relative concentrations of the La@C$_{74}$ isomers computed with the B3LYP/6–311G*~sdd energetics, B3LYP/3-21G~dz entropy, and RRHO (left) or FEM (right) treatment.
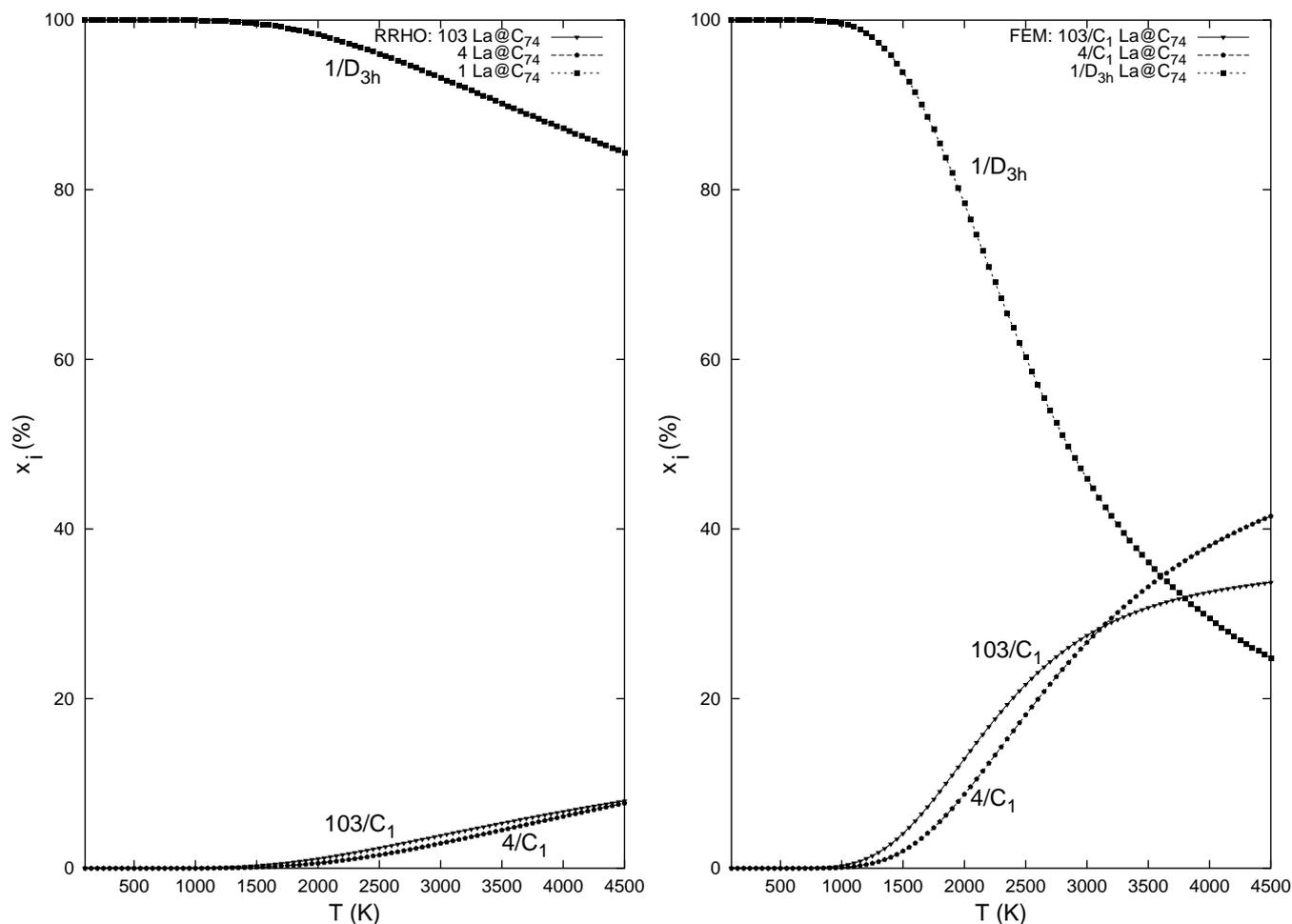

Figure 5. B3LYP/3-21G~dz optimized structures of the three most populated La@C$_{76}$ isomers.


6247   6244 T_d IPR
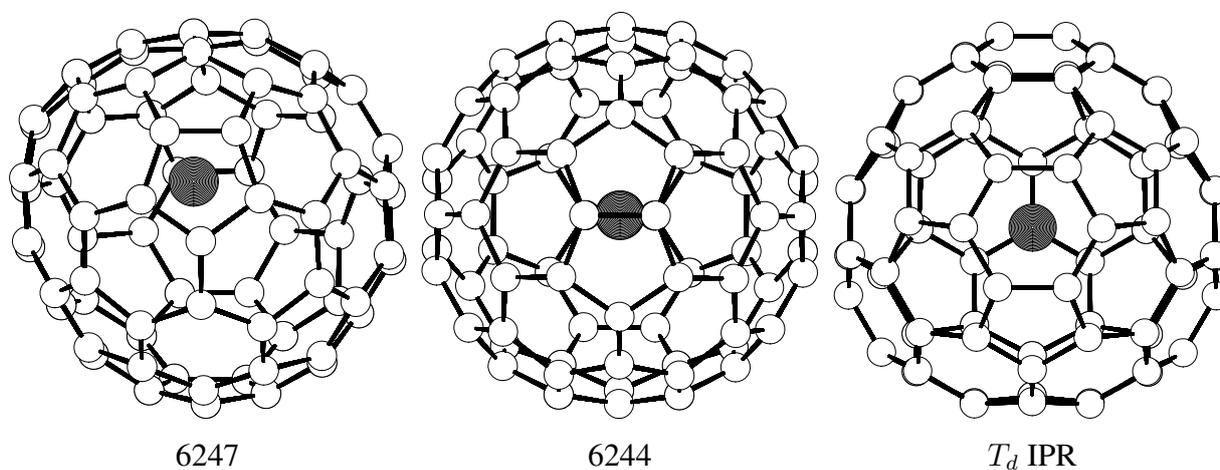
Table 2. La@C$_{76}$ relative potential energies $\Delta E_{pot,rel}$ computed [a] in the B3LYP/3–21G$\sim$dz optimized geometries.

Species [b]	$\Delta E_{pot,rel}$	(kcal/mol)
	B3LYP/3–21G$\sim$dz	B3LYP/6–31G*$\sim$dz[c]
6727	15.86	19.46
1603	12.26	17.76
6247	10.00	13.22
6244	6.90	7.36
T_d IPR	0	0

[a] See the text for the abbreviations; [b] See Figure 5; [c] In the B3LYP/6-31G*$\sim$dz optimized geometry.

Figure 6. Relative concentrations of the La@C$_{76}$ isomers computed with the B3LYP/6-31G*$\sim$dz energetics, B3LYP/3-21G$\sim$dz entropy, and FEM treatment.
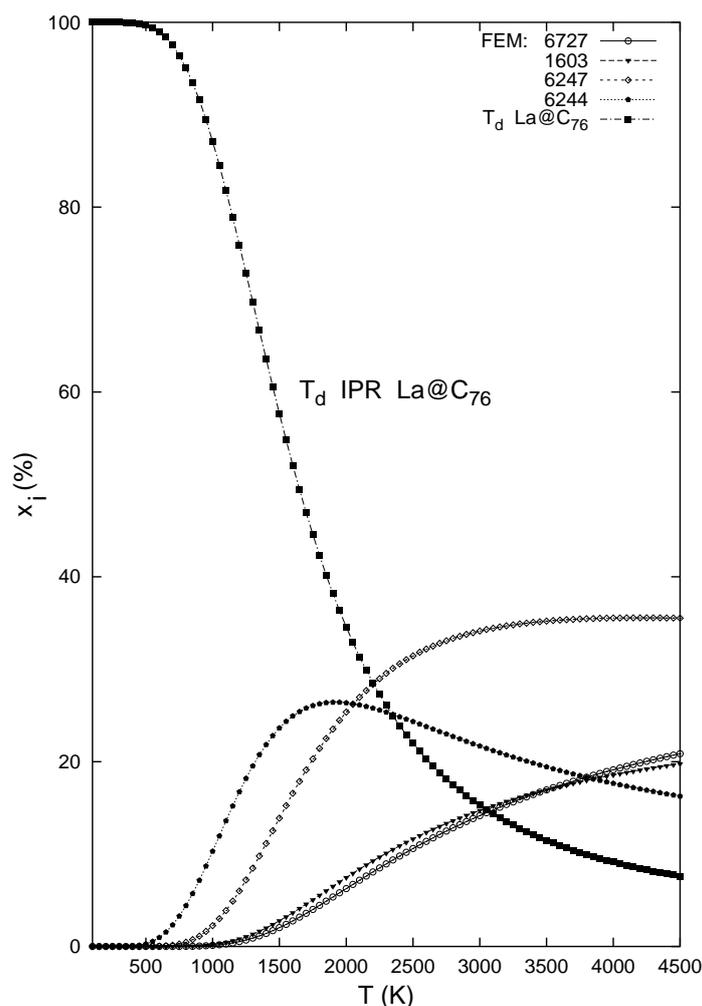
Various endohedral cage compounds have been suggested as possible candidate species for molecular memories and other future nanotechnological applications. One approach is built on endohedral species

with two possible location sites of the encapsulated atom [43] while another concept of quantum computing aims at a usage of spin states [44] or fullerene-based molecular transistors [45]. For the first memory concept, the otherwise low potential barriers for a three-dimensional rotational motion of encapsulates in the cages [46,47] could be restricted by an additional cage derivatization [41]. Obviously, a further accumulation of knowledge on endohedral properties is needed, both computed [48–53] and observed [54–56], before such applications can be truly explored.

4. Conclusions

The computational study shows that while La@C_{72} is dominated by non-IPR cages and in La@C_{74} the IPR moiety prevails, for La@C_{76} a non-IPR cage should be present as a minor isomer. The sensitivity of the computed populations to the symmetry treatment is also highlighted.

Acknowledgements

References

1. Achiba, Y.; Kikuchi, K.; Aihara, Y.; Wakabayashi, T.; Miyake, Y.; Kainosho, M. Trends in Large Fullerenes: Are They Balls or Tubes. In *The Chemical Physics of Fullerenes 10 (and 5) Years Later*; Andreoni, W., Ed.; Kluwer Academic Publishers: Dordrecht, Netherlands, 1996; pp. 139–147.

2. Diener, M.; Alford, J. Isolation and properties of small-bandgap fullerenes. *Nature* **1998**, *393*, 668–671.

3. Ichikawa, T.; Kodama, T.; Suzuki, S.; Fujii, R.; Nishikawa, H.; Ikemoto, I.; Kikuchi, K.; Achiba, Y. Isolation and characterization of a new isomer of Ca@C_{72}. *Chem. Lett.* **2004**, *33*, 1008–1009.

4. Wakahara, T.; Nikawa, H.; Kikuchi, T.; Nakahodo, T.; Rahman, G.M.A.; Tsuchiya, T.; Maeda, Y.; Akasaka, T.; Yoza, K.; Horn, E.; *et al*. La@C_{72} having a non-IPR carbon cage. *J. Am. Chem. Soc.* **2006**, *128*, 14228–14229.

5. Wan, T.; Zhang, H.; Nakane, T.; Xu, Z.; Inakuma, M.; Shinohara, H.; Kobayashi, K.; Nagase, S. Production, isolation, and electronic properties of missing fullerenes: Ca@C_{72} and Ca@C_{74}. *J. Am. Chem. Soc.* **1998**, *120*, 6806–6807.

6. Okazaki, T.; Lian, Y.; Gu, Z.; Suenaga, K.; Shinohara, H. Isolation and spectroscopic characterization of Sm-containing metallofullerenes. *Chem. Phys. Lett.* **2000**, *320*, 435–440.

7. Haufe, O.; Hecht, M.; Grupp, A.; Mehring, M.; Jansen, M. Isolation and spectroscopic characterization of new endohedral fullerenes in the size gap of C_{74} to C_{76}. *Z. Anorg. Allgem. Chem.* **2005**, *631*, 126–130.

8. Reich, A.; Panthofer, M.; Modrow, H.; Wedig, U.; Jansen, M. The structure of $Ba@C_{74}$. *J. Am. Chem. Soc.* **2004**, *126*, 14428–14434.

9. Chai, Y.; Guo, T.; Jin, C.; Haufler, R.; Chibante, L.; Fure, J.; Wang, L.; Alford, J.; Smalley, R. Fullerenes with Metals Inside. *J. Phys. Chem.* **1991**, *95*, 7564–7568.

10. Nikawa, H.; Kikuchi, T.; Wakahara, T.; Nakahodo, T.; Tsuchiya, T.; Rahman, G.; Akasaka, T.; Maeda, Y.; Yoza, K.; Horn, E.; *et al.* Missing metallofullerene $La@C_{74}$. *J. Am. Chem. Soc.* **2005**, *127*, 9684–9685.

11. Matsuoka, H.; Ozawa, N.; Kodama, T.; Nishikawa, H.; Ikemoto, I.; Kikuchi, K.; Furukawa, K.; Sato, K.; Shiomi, D.; Takui, T.; *et al.* Multifrequency EPR study of metallofullerenes: $Eu@C_{82}$ and $Eu@C_{74}$. *J. Phys. Chem. B* **2004**, *108*, 13972–13976.

12. Xu, J.; Lu, X.; Zhou, X.; He, X.; Shi, Z.; Gu, Z. Synthesis, isolation, and spectroscopic characterization of ytterbium-containing metallofullerenes. *Chem. Mater.* **2004**, *16*, 2959–2964.

13. Stevenson, S.; Dorn, H.; Burbank, P.; Harich, K.; Haynes, J.; Kiang, C.; Salem, J.; de Vries, M.; van Loosdrecht, P.; Johnson, R.; *et al.* Automated HPLC separation of endohedral metallofullerene $Sc@C_{2n}$ and $Y@C_{2n}$ Fractions. *Anal. Chem.* **1994**, *66*, 2675–2679.

14. Tagmatarchis, N.; Aslanis, E.; Prassides, K.; Shinohara, H. Mono-, di- and trierbium endohedral metallofullerenes: Production, separation, isolation, and spectroscopic study. *Chem. Mater.* **2001**, *13*, 2374–2379.

15. Moro, L.; Ruoff, R.; Becker, C.; Lorents, D.; Malhotra, R. Studies of metallofullerene primary soots by laser and thermal-desorption mass-spectrometry. *J. Phys. Chem.* **1993**, *97*, 6801–6805.

16. Okubo, S.; Kato, T.; Inakuma, M.; Shinohara, H. Separation and characterization of ESR-active lanthanum endohedral fullerenes. *New Diam. Front. Carbon Technol.* **2001**, *11*, 285–294.

17. Fowler, P.W.; Manolopoulos, D.E. *An Atlas of Fullerenes*; Clarendon Press: Oxford, UK, 1995.

18. Kobayashi, K.; Nagase, S.; Yoshida, M.; Osawa, E. Endohedral metallofullerenes. Are the isolated pentagon rule and fullerene structures always satisfied? *J. Am. Chem. Soc.* **1997**, *119*, 12693–12694.

19. Nagase, S.; Kobayashi, K.; Akasaka, T. Unconventional cage structures of endohedral metallofullerenes. *J. Mol. Struct. (Theochem)* **1999**, *461–462*, 97–104.

20. Kobayashi, K.; Nagase, S. Structures and Electronic Properties of Endohedral Metallofullerenes: Theory and Experiment. In *Endofullerenes – A New Family of Carbon Clusters*; Akasaka, T., Ed.; Kluwer Academic Publishers: Dordrecht, The Netherlands, 2002; pp. 99–119.

21. Slanina, Z.; Kobayashi, K.; Nagase, S. $Ca@C_{72}$ IPR and non-IPR structures: Computed temperature development of their relative concentrations. *Chem. Phys. Lett.* **2003**, *372*, 810–814.

22. Slanina, Z.; Kobayashi, K.; Nagase, S. $Ca@C_{74}$ isomers: Relative concentrations at higher temperatures. *Chem. Phys.* **2004**, *301*, 153–157.

23. Tang, C.; Yuan, Y.; Deng, K.; Liu, Y.; Li, X.; Yang, J.; Wang, X. Geometric and electronic properties of endohedral $Si@C_{74}$. *J. Chem. Phys.* **2006**, 104307.

24. Slanina, Z.; Uhlik, F.; Nagase, S. Computed structures of two known Yb@C_{74} isomers. *J. Phys. Chem. A* **2006**, *110*, 12860–12863.

25. Slanina, Z.; Uhlik, F.; Lee, S.L.; Adamowicz, L.; Nagase, S. Computations on Three Isomers of La@C_{74}. *Int. J. Quantum Chem.* **2008**, *108*, 2636–2640.

26. Slanina, Z.; Uhlik, F.; Adamowicz, L.; Nagase, S. Computational screening of metallofullerenes for nanoscience: Sr@C_{74}. *Mol. Simul.* **2008**, *34*, 17–21.

27. Slanina, Z.; Uhlik, F. Temperature-dependence of the gibbs energy ordering of isomers of Cl_2O_2. *J. Phys. Chem.* **1991**, *95*, 5432–5434.

28. Slanina, Z.; Uhlik, F.; Zhao, X.; Osawa, E. Enthalpy-entropy interplay for C_{36} cages: B3LYP/6-31G(*) calculations. *J. Chem. Phys.* **2000**, *113*, 4933–4937.

29. Slanina, Z.; Kobayashi, K.; Nagase, S. Computed temperature development of the relative stabilities of La@C_{82} isomers. *Chem. Phys. Lett.* **2004**, *388*, 74–78.

30. Slanina, Z.; Nagase, S. Stability computations for Ba@C_{74} isomers. *Chem. Phys. Lett.* **2006**, *422*, 133–136.

31. Becke, A. Density-functional thermochemistry 3. The role of exact exchange. *J. Chem. Phys.* **1993**, *98*, 5648–5652.

32. Lee, C.; Yang, W.; Parr, R. Development of the colle-salvetti correlation-energy formula into a functional of the electron-density. *Phys. Rev. B* **1988**, *37*, 785–789.

33. Hay, P.; Wadt, W. Ab initio effective core potentials for molecular calculations-potentials for K to Au including the outermost core orbitals. *J. Chem. Phys.* **1985**, *82*, 299–310.

34. Frisch, M.J.; Trucks, G.W.; Schlegel, H.B.; Scuseria, G.E.; Robb, M.A.; Cheeseman, J.R.; Montgomery, J.A., Jr.; Vreven, T.; Kudin, K.N.; Burant, J.C.; *et al.* *Gaussian 03, Revision C.01*; Gaussian, Inc.: Wallingford, CT, USA, 2004.

35. Cao, X.; Dolg, M. Segmented contraction scheme for small-core lanthanide pseudopotential basis sets. *J. Mol. Struct. (Theochem)* **2002**, *581*, 139–147.

36. Slanina, Z. Equilibrium isomeric mixtures-potential-energy hypersurfaces as the origin of the overall thermodynamics and kinetics. *Int. Rev. Phys. Chem.* **1987**, *6*, 251–267.

37. Cross, R.; Saunders, M. Transmutation of fullerenes. *J. Am. Chem. Soc.* **2005**, *127*, 3044–3047.

38. Slanina, Z.; Adamowicz, L. On the relative stabilities of dodecahedron-shaped and bowl-shaped structures of C_{20}. *Thermochim. Acta* **1992**, *205*, 299–306.

39. Slanina, Z.; Adamowicz, L.; Kobayashi, K.; Nagase, S. Gibbs energy-based treatment of metallofullerenes: Ca@C_{72}, Ca@C_{74}, Ca@C_{82}, and La@C_{82}. *Mol. Simul.* **2005**, *31*, 71–77.

40. Akasaka, T.; Nagase, S.; Kobayashi, K.; Walchli, M.; Yamamoto, K.; Funasaka, H.; Kako, M.; Hoshino, T.; Erata, T. C-13 and La-139 NMR studies of La_2@C_{80}: First evidence for circular motion of metal atoms in endohedral dimetallofullerenes. *Angew. Chem. Intl. Ed. Engl.* **1997**, *36*, 1643–1645.

41. Kobayashi, K.; Nagase, S.; Maeda, Y.; Wakahara, T.; Akasaka, T. La_2@C_{80}: Is the circular motion of two La atoms controllable by exohedral addition? *Chem. Phys. Lett.* **2003**, *374*, 562–566.

42. Slanina, Z.; Lee, S.L.; Uhlik, F.; Adamowicz, L.; Nagase, S. Computing relative stabilities of metallofullerenes by Gibbs energy treatments. *Theor. Chem. Acc.* **2007**, *117*, 315–322.

43. Gimzewski, J.K. Scanning Tunneling and Local Probe Studies of Fullerenes. In *The Chemical Physics of Fullerenes 10 (and 5) Years Later*; Andreoni, W., Ed.; Kluwer Academic Publishers: Dordrecht, The Netherlands, 1996; pp. 117–136.

44. Harneit, W.; Waiblinger, M.; Meyer, C.; Lips, K.; Weidinger, A. Concept for Quantum Computing with $N@C_{60}$. In *Recent Advances in the Chemistry and Physics of Fullerenes and Related Materials, Volume 11, Fullerenes for the New Millennium*; Kadish, K. M., Kamat, P. V., Guldi, D., Eds.; Electrochemical Society: Pennington, NJ, USA, 2001; pp. 358–361.

45. Hiroshiba, N.; Tanigaki, K.; Kumashiro, R.; Ohashi, H.; Wakahara, T.; Akasaka, T. C_{60} field effect transistor with electrodes modified by $La@C_{82}$. *Chem. Phys. Lett.* **2004**, *400*, 235–238.

46. Heine, T.; Vietze, K.; Seifert, G. C-13 NMR fingerprint characterizes long time-scale structure of $Sc_3N@C_{80}$ endohedral fullerene. *Mag. Res. Chem.* **2004**, *42*, S199–S201.

47. Slanina, Z.; Nagase, S. $Sc_3N@C_{80}$: Computations on the two-isomer equilibrium at high temperatures. *ChemPhysChem* **2005**, *6*, 2060–2063.

48. Liu, D.; Hagelberg, F. Impact of internal electron transfer on the structure of C_{74} encapsulating Sc and La metal atom impurities. *Int. J. Quant. Chem.* **2007**, *107*, 2253–2260.

49. Slanina, Z.; Ishimura, K.; Kobayashi, K.; Nagase, S. C_{72} isomers: The IPR-satisfying cage is disfavored by both energy and entropy. *Chem. Phys. Lett.* **2004**, *384*, 114–118.

50. Uhlik, F.; Slanina, Z.; Nagase, S. $Mg@C_{74}$ isomers: Calculated relative concentrations and comparison with $Ca@C_{74}$. *Phys. Status Solidi A* **2007**, *204*, 1905–1910.

51. Slanina, Z.; Uhlik, F.; Lee, S.L.; Adamowicz, L.; Nagase, S. Computed structures and relative stabilities of $Be@C_{74}$. *Int. J. Quant. Chem.* **2007**, *107*, 2494–2498.

52. Slanina, Z.; Zhao, X.; Kurita, N.; Gotoh, H.; Uhlik, F.; Rudzinski, J.; Lee, K.; Adamowicz, L. Computing the relative gas-phase populations of C_{60} and C_{70}: Beyond the traditional $\Delta H^o_{f,298}$ scale. *J. Mol. Graphics Mod.* **2001**, *19*, 216–221.

53. Slanina, Z.; Lee, S.; Adamowicz, L.; Uhlik, F.; Nagase, S. Computed structure and energetics of $La@C_{60}$. *Int. J. Quant. Chem.* **2005**, *104*, 272–277.

54. Rodriguez-Fortea, A.; Balch, A.L.; Poblet, J.M. Endohedral metallofullerenes: A unique host-guest association. *Chem. Soc. Rev.* **2011**, *40*, 3551–3563.

55. Osuna, S.; Swart, M.; Sola, M. The reactivity of endohedral fullerenes. What can be learnt from computational studies? *Phys. Chem. Chem. Phys.* **2011**, *13*, 3585–3603.

56. Yang, S.; Liu, F.; Chen, C.; Jiao, M.; Wei, T. Fullerenes encaging metal clusters-clusterfullerenes. *Chem. Commun.* **2011**, *47*, 11822–11839.